

# An unsupervised approach for subpixelic land-cover change detection

Amandine Robin\*, Lionel Moisan\* and Sylvie Le Hégarat-Masclé†

\*Université Paris Descartes, MAP5 (CNRS UMR 8145), France

Email: Amandine.Robin@math-info.univ-paris5.fr,

Lionel.Moisan@math-info.univ-paris5.fr

†Université Paris-Sud, IEF (CNRS UMR 8622), France

Email: le-hegar@ief.u-psud.fr

**Abstract**—In this paper, we present a new method for subpixelic land-cover change detection using coarse resolution time series, as they offer a high time-repetitiveness of acquisition. Changes are detected by analyzing the coherence between a coarse resolution time series and a high resolution classification as a description of the land-cover state at the date of reference. To that aim, an a-contrario model is derived, leading to the definition of a probabilistic coherence criterion free of parameter and free of any *a priori* information. This measure is the core of a stochastic algorithm that selects automatically the image sub-domain representing the most likely changes. Some particular problems related to the use of time series are discussed, such as the potential high variability of a time series or the problem of missing data. Some experiments are then presented on pseudo-actual data, showing a good performance for change detection and a high robustness to the considered resolution ratio (between the high resolution classification and the coarse resolution time series).

## I. INTRODUCTION

In this paper, we focus on the problem of change detection for applications such as vegetation monitoring or classification updates. In this context, a high frequency of data acquisition is often required, leading usually to the use of coarse spatial resolution time series. In the image processing literature, the problem of change detection has been widely explored (*e.g.* for video applications) but some specific difficulties appear dealing with remote sensed data. Indeed, illumination variations, soil moisture, differences of sensor calibration between two dates, absence of *a priori* information on expected changes or misregistration are factors to take into account, since even after specific pre-processing (*e.g.* radiometric or geometric corrections) they usually persist partly. Moreover, if a high frequency of acquisition is mandatory for vegetation monitoring, spatial resolution is also necessary in order to locate objects of interest. As the remote sensed images dedicated to vegetation can not be acquired with both a high spatial resolution and a high temporal frequency, we choose high temporal frequency and try to detect subpixelic land-cover changes, by comparing a coarse resolution (CR) time series to a former high resolution (HR) reference classification. Indeed, such a comparison allows to follow objects that are observable in the HR classification but impossible to distinguish at a coarse resolution. The classification is hence used as a mask

enabling to study the coherence between the time series and the classification.

According to the linear mixture model (*cf.* [1]), the expectation of the measurement performed over a mixed pixel is the average of the measure corresponding to each class weighted by its occupation rate in the pixel. The value observed within a CR pixel  $x$  at a date  $t$  can hence be estimated by

$$\hat{v}(x, t) = \sum_l \alpha_l(x) \mu_l(t), \quad (1)$$

where  $\alpha_l(x)$  denotes the relative area of the CR pixel  $x$  occupied by the label  $l$  (by construction,  $\sum_{l \in L} \alpha_l(x) = 1$ ) and  $\mu_l(t)$  represents the average intensity characterizing each label at date  $t$ . As the problem we consider assumes that a HR classification is given at the date of reference, the class proportions  $\alpha_l(x)$  are known.

Let  $\Omega$  denote the image domain,  $\mathcal{T}$  the set of acquisition dates, and  $\omega$  a spatio-temporal sub-domain of  $\Omega \times \mathcal{T}$ . The minimal residual error between observations and the reconstruction obtained from a given label distribution and the classification image can be measured over a sub-domain  $\omega \subset \Omega \times \mathcal{T}$  using the squared Euclidean norm by

$$E_\omega = \min_\mu \|v_\omega - \hat{v}_\omega\|_2^2, \quad (2)$$

where  $v_\omega$  is the CR time series restricted to the sub-domain  $\omega$ . An estimation of the mean values  $\mu_t(l)$  is then obtained through the minimal argument of the residual error.

At this stage, the main detection issue is the definition of an *a priori* threshold on the residual error  $E_\omega$ , in order to decide between changes and no-changes. This threshold should be an appropriate combination of the residual error  $E_\omega$  and the size of the sub-domain  $\omega$ , since even without changes, larger sub-domains are expected to yield larger residual errors since they involve more pixels.

In section II-A, we build an a-contrario detection model that enables to combine these parameters in a single probabilistic criterion allowing the detection of the most coherent sub-domain with a given classification (that is, a given high-resolution label map), controlling the expected number of false alarms. The complementary of this sub-domain is then considered as the set of pixels about to represent changes. Performances resulting from a theoretical study of the model

according to its main parameters are also mentioned. Some numerical issues are raised in Section II-B and a stochastic RANSAC algorithm is described. Finally, some results are presented for an agricultural site of the Danubian plain (Rumania, ADAM database).

## II. PROPOSED CHANGE DETECTION METHOD

### A. *a-contrario* model

The *a-contrario* detection (see [2], [3]) enables to compute a level of significance without modeling changes nor quantifying the expected differences (noise, distortions, intrinsic variability, etc.), *i.e.* with very few *a priori* information. It relies on the idea that a given structure is to be detected if its occurrence is a very unlikely event according to a naive random model on the data. In the context of change detection, this idea is particularly interesting as changes cannot be reasonably modeled through a list of all possible changes (crop rotation, forest cuts or fires can occur on the Earth surface with various size and radiometric intensities). Moreover, an *a priori* model of the no-change surface is also physically difficult to define as temporal evolution profiles of different land-covers vary from a year to another and from a geographical area to another. Approaches based on the comparison of temporal profiles from a year to another can be found in the literature [4]–[6], but they face the threshold choice issue we mentioned earlier.

Following the general framework of *a-contrario* modeling, let us assume as a naive model ( $H_0$ ) that a CR image  $v$  is a random field  $V$  of  $|\Omega|$  independent Gaussian centered variables with a given variance  $\sigma^2$ . Let us recall that the ambition of this model is not to reasonably model the data but rather to define a noise model against which we will detect significant structures in the data. From there, we define the coherence measure of a spatial sub-domain  $\omega$  by

$$NFA(\omega, E_\omega) = \eta(|\omega|) \cdot \mathbb{P}_{H_0}(E_\omega), \quad (3)$$

where  $\eta$  is a normalization term and  $\mathbb{P}_{H_0}(E_\omega)$  represents the probability of measuring as surprisingly small error by chance on the sub-domain  $\omega$ , that is, after computation,

$$\mathbb{P}_{H_0}(E_\omega) = \frac{1}{\Gamma(\frac{|\omega|-L}{2})} \int_0^{E_\omega/2\sigma^2} e^{-t} t^{\frac{|\omega|-L}{2}-1} dt, \quad (4)$$

where  $\Gamma$  is the usual Euler function. The function  $\eta$  is chosen in order to ensure that the expected number of false alarms remains as small as desired. Several choices are then acceptable. In this study, it is set to  $\eta = |\Omega| \binom{|\omega|}{|\Omega|}$  as this choice enables to distribute the risk uniformly with respect to the domain size, and it guarantees an average number of false detections less than 1. This choice permits the comparison of sub-domains of various size.

Let us remark that this measure depends on the size of the considered sub-domain, on the number of labels in the classification and on the naive model variance. All these parameters are obtained directly from the data, except the variance  $\sigma^2$  which can be chosen arbitrary. It has been set to the empirical variance of the data series, leading to a model

free of parameters meanwhile ensuring less than one detection by chance in a white noise image.

From a theoretical point of view, an analysis of the detection model was performed to understand the influence of the size and the level of contrast of the data [7]. First, it has been confirmed that the higher the time series contrast is, the higher is the coherence measure between a HR classification and a CR time series (and any amount of changes can be detected if the data contrast is high enough). Moreover, for any given level of contrast, any amount of changes can be detected as soon as the data size is large enough. As the contrast and the amount of changes are typically presented as limiting factors in the literature, these results offer promising possibilities for the applicability of the proposed approach.

Using the coherence measure (3), the sub-domain of changes can be seen as the complementary sub-domain of the one that maximizes the coherence between a given classification and a CR time series (the one that minimizes the *NFA* value). Next section presents the algorithm used for this research.

### B. Numerical aspects

From the coherence measure (3), a sub-domain is detected as coherent with a given label map if it corresponds to the sub-domain that minimizes the value of the *NFA*. The latter depends on the size of the CR image, the number of labels  $L$ , the size of the considered sub-domain  $|\omega|$ , the standard deviation of the naive model  $\sigma$  and the cumulated quadratic residue on this sub-domain  $E_\omega$ . All *NFA* parameters can be obtained directly from the data except the cumulated quadratic residue  $E_\omega$  which depends on the class' means, which is *a priori* unknown. It is hence necessary to estimate the mean characteristics of each class before being able to compute the quadratic residues associated to a considered sub-domain and then the corresponding *NFA*. The mean estimation and the detection itself are two linked problems as the quality of estimation has a strong impact on the performance of the detection.

Practically, the algorithm takes a HR classification and a CR time series as inputs and returns the sub-domain  $\omega$  leading to the smallest value of *NFA* as an estimate of the most unchanged domain. It is fully unsupervised as all parameters are obtained directly from the data. The algorithm is based on a RANSAC strategy (*cf.* [8]) for pixel selection. This strategy is combined with the *a-contrario* model to compose a robust change detection method. Indeed, an empirical analysis of the robustness has shown that up to 75% of outliers (*e.g.* change pixels) can be well detected. This performance is particularly high compared to the usual limitation threshold of 25% or 30% for change pixels found in the literature (*cf.* [9]). It shows that the method we present here is very robust to the amount of changes or outliers, confirming the asymptotic theoretical result mentioned Section II-A. Moreover, another empirical analysis has shown that changes impacting more than 20% of a CR pixel are detected with less than 3% (median) of error and that performances are stable with respect to the resolution

ratio (the impacting factor being the occupation rate within a CR pixel). The algorithm in the case where a single CR image  $v$  is used is detailed in the following.

- Assign  $\sigma^2$  to the CR image variance.
- Initialize  $\delta_{min}[]$ ,  $NFA[]$  and  $NFA_{min}$  to  $+\infty$ .
- Repeat  $N$  times
  - 1) draw a random set  $I$  of  $L$  CR pixels  $x$ ,
  - 2) estimate the label mean vector  $\mu$  from equations
 
$$v(x) = \sum_l \alpha_l(x) \mu_l,$$
 defined for  $x \in I$ ,
  - 3) compute  $E(x) = (v(x) - \sum_l \alpha_l(y) \mu_l)^2$ , for  $x \in \mathcal{D}_{BR}$ ,
  - 4) sort  $\mathcal{D}_{BR}$  into a vector  $(x_i)_{1 \leq i \leq |\mathcal{D}_{BR}|}$  by increasing error  $E(x_i)$ .
  - 5) initialize  $\delta = \sum_{i=0}^L E(x_i)$ ,
  - 6) for each index  $i \in \{L+1, \dots, |\mathcal{D}_{BR}|\}$ ,
    - set  $\delta = \delta + E(x_i)$ ,
    - if  $\delta < \delta_{min}[i]$  then
      - \* set  $\delta_{min}[i] = \delta$ ,
      - \* compute the corresponding  $NFA[i]$  value,
      - \* if  $NFA[i] \leq NFA_{min}$ , then
        - set  $NFA_{min} = NFA[i]$
        - set  $D = \{x_k\}_{k=1..i}$
      - \* end if
    - end if
  - 7) end for
- end repeat

The research of the minimum  $NFA$  has been optimized remarking that, for a given image, the  $NFA$  does not depend directly on the sub-domain of interest  $\omega$  but only of its cardinal and, monotonously, on cumulated quadratic errors on  $\omega$ . Sorting the pixel values by increasing quadratic errors hence enables to minimize the  $NFA$  over all  $|\Omega|!$  sub-domains by increasing only  $|\Omega|$  sub-domains, with an overall complexity  $O(|\Omega| \log |\Omega|)$ .

Moreover, notice that the only parameter of the algorithm is the number of iterations ( $N$ ). Due to RANSAC strategy, convergence requires a very high number of iterations ( $N = 100\,000$  in the following experiments). However, this is not really a limiting factor as the computation time of each iteration is very fast (for instance, 100,000 iterations for change detection considering a HR classification of size  $256 \times 256$  and a CR image of size  $16 \times 16$  takes about 10s on a laptop).

### III. APPLICATION TO TIME SERIES

In the multitemporal case, different approaches may be chosen depending whether the application requires the detection of a spatio-temporal sub-domain or a spatial sub-domain. For instance, a sequential approach can be considered, comparing the minimum  $NFA$  values obtained for each image separately. Such an approach could be used in order to find the image of a time series which is the most coherent with the classification

but it does not permit to detect a spatio-temporal sub-domain since it does not take into account the whole time series. In practice, time series are rather used to analyse the temporal evolution of intensities and to enable the detection of spatio-temporal domains, which may be useful since changes can occur at some dates without impacting other ones.

In this work, a vectorial approach is considered for the detection of a spatio-temporal sub-domain of changes, assuming that all images of the time series are accurately registered. Denote  $\mathcal{T}$  the set of acquisition dates of a time series. The a-contrario detection model presented Section II-A can be easily extended to time series, considering a spatio-temporal sub-domain  $\Omega \times \mathcal{T}$ . In this section,  $\omega$  denote a spatio-temporal sub-domain of  $\Omega \times \mathcal{T}$ . As a naive model, the CR time series is assumed to be a random field of  $|\Omega| \times |\mathcal{T}|$  independent Gaussian random variables of zero-mean and variance  $\sigma^2$ . From there, a  $NFA$  can be defined by

$$NFA(\omega, E_\omega) = \eta(|\omega|) \cdot \mathbb{P}_{H_0}(E_\omega), \quad (5)$$

where  $\eta(|\omega|) = |\Omega| \times |\mathcal{T}| \binom{|\omega|}{|\Omega| \times |\mathcal{T}|}$  and

$$\mathbb{P}_{H_0}(E_\omega) = \frac{1}{\Gamma(\frac{|\omega| - L \times T}{2})} \int_0^{E_\omega/2\sigma^2} e^{-t} t^{\frac{|\omega| - L \times T}{2} - 1} dt. \quad (6)$$

Concerning the choice of the variance of the naive model, let us recall that, in the monotemporal case, taking the CR image variance as the variance of the naive model was justified by the fact that nothing should be detected in a white noise image. In the multitemporal case, setting the variance of the naive model to the variance of the CR time series does not ensure this property anymore as, in the case of high variance differences between dates within the time series, such a naive model could detect noisy pixels as coherent. Hence, the use of this naive model can lead to the false detection of noisy pixels or to the complete validation of very different classifications. To avoid the detection of irrelevant sub-domains, the intensity values are normalized by the image variance within each image and the variance of the naive model is set to 1. This choice enables to give an equal weight to all images of the series.

The multitemporal algorithm is very close to the monotemporal one but the fact that time series may contain missing data at different locations for each date must be taken into account in the research of the sub-domain of changes. A simple possibility is to restrict the study to the set of pixels that are validated for all dates but this might considerably reduce the analysed domain.

Instead, we propose to consider a restriction of  $\Omega \times \mathcal{T}$  to the set of valid pixels. More precisely, each pixel of the spatial domain is considered as a vector whose coordinates correspond to each of its valid dates. This way, if a pixel is impacted by some changes at a given date, it will be rejected from the whole series. In order to allow the comparison of sub-domains of different size for each date, the cumulated residues are normalized by the number of valid dates, leading to a mean cumulated residue. From there, the same algorithm as in Section II-B can be used.

Figure 1 shows the evolution of the  $NFA$  values obtained from a time series as a function of the number of labels chosen for the HR classification. In this example, the HR classification has been estimated in some way (see [7], [10] for details) from the whole time series (8 images), for a number of classes of 1 to 20. Comparing a part of this time series to the HR classification, we expect to validate the whole spatio-temporal domain. Each curve presented Figure 1 corresponds to the value obtained of the time series from the first  $T$  dates. Let us remark that the use of one date alone does not permit to validate classifications while using any time series containing more than one date enables to validate the whole domain. Moreover, each curve shows a minimum value for 12 labels, meaning that the 12 classes classification is the most coherent with the time series.

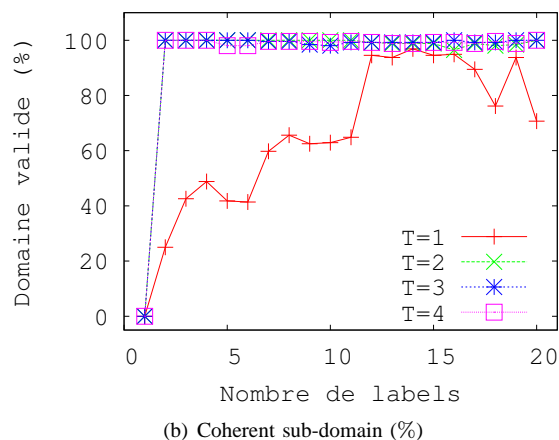
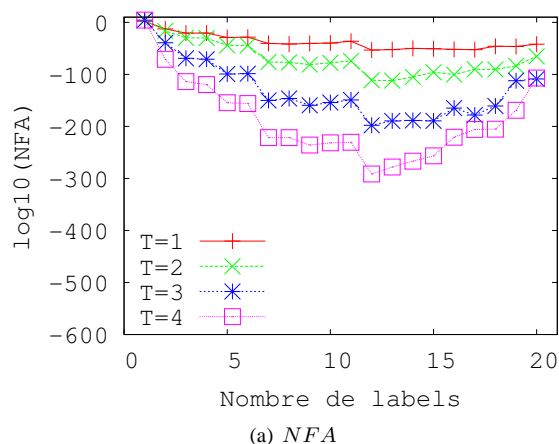


Fig. 1. Results obtained using the first  $T$  dates of the time series (figure 2 (b)) and a classification realized using the whole time series (of 8 dates) for 1 to 20 classes. The  $\log_{10}(NFA)$  value (a) and the relative size (b) of the most coherent sub-domain are plotted in function of the number of classes. Each curve corresponds to the results obtained for a given subset of the time series (first  $T$  dates). All HR classifications are validated as soon as at least 2 dates are used, but not for a single date.

The multitemporal detection algorithm takes a HR classification and a CR time series as inputs, and returns the spatio-temporal CR sub-domain which is the most coherent with the HR classification. In this section, some results obtained using actual HR images (SPOT4) of the Danubian Plain (Rumania, ADAM database) are presented, while the CR time series has been simulated by averaging HR images on pixel blocks of size  $15 \times 15$  (Figure 2 (b)). As no groundtruth on changes were available, a HR classification has been created for 10 labels and using 8 HR actual images (Figure 2 (a)). The change detection method applied to this classification and the corresponding CR time series of 8 dates enabled to validate the whole domain except the dark pixel of Figure 2 (c). We then introduced different changes artificially in the HR classification. In Figure 2, changes were introduced in the reference classification by replacing a random selection of segments label with another existing label. Figure 2(d) to (f) presents several cases of such simulated changes and pixels detected as changes are presented in red in the CR domain. On the same image, the boundary of each segment is traced in black, pixels corresponding to simulated changes are represented in green and those that were already detected in (c) are in pink. The hint of segments enables to visualize the impact area of segments of interest within CR pixels. Changes are well detected by the method, even when they impact a very small area of a CR pixel (Figure 2(a) and (c)). In order to simulate the appearance of a new class, Figure 3(a) to (c) shows the results obtained using classification (a) modified by attribution of a new class to selected segments. Changes are still well detected, except in figure 3(a) and (b) where one pixel (in the middle of the bottom line) has been overdetected. This last overdetection is probably due to the fact a minority class has been modified to simulate a change, leaving very few or no occurrence of the same class.

In order to consider some other type of changes, let us consider the HR Classification Figure 3 (a) and the corresponding CR image Figure 3 (b) where changes have been simulated (see in the white area Figure (c)). The method applied to Figures (a) and (b) enabled to detect all red pixels Figure (c). Pink pixels correspond to pixels that were already detected before the simulation of changes in (b).

An important aspect of this method is the resolution ratio between HR and CR. The comparison of the results presented Figure 4 shows the robustness of the method with respect to the resolution ratio. Indeed, in a monotemporal context, the change detection method has been applied for the validation of the classification shown on Figure 3 (a) from a CR image obtained by averaging HR images by blocks of size  $5 \times 5$  (Figure 4(a)),  $15 \times 15$  (Figure 4(b)) and  $50 \times 50$  (Figure 4(c)). In these three cases, about 4.5% of the pixels are detected. Let us remark that the spatial location of the detected pixels as non-coherent (in red) is stable, showing the good robustness of the method with respect to the resolution ratio.

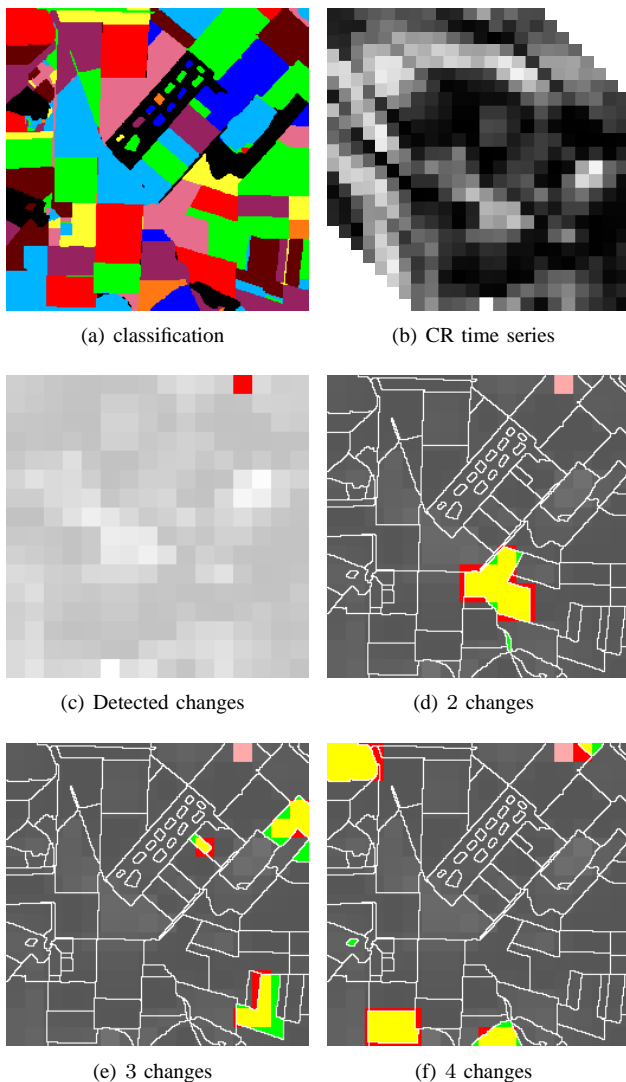


Fig. 2. Results obtained for changes introduced in the classification by a random sort of 3, 4 or 5 segments, and a new label for the sorted segments. The label is sorted between 1 and  $L$ . Changes that have been simulated in the classification are represented in yellow when they are detected, green otherwise. Detected pixels that do not correspond to changes are represented in pink if they were already detected before the simulation of changes (cf. (c)) and in red otherwise. Globally, remark that simulated changes are well detected even when they impact a weak proportion of a CR pixel. On Figure (c), a missed detection can be observed (top right, in green).

## V. CONCLUSION

In this paper, an a-contrario model has been proposed for subpixelic change detection in land-cover coarse resolution time series, by defining a coherence measure of an image sub-domain according to the knowledge of a high resolution classification at a reference date. The model provides an explicit function combining all detection parameters into a single level of coherence, thus yielding an unsupervised detection method. A stochastic algorithm using a RANSAC strategy has also been described in the monotemporal case.

In the multitemporal case, the problem of missing data has been discussed and an adapted extension of the algorithm has

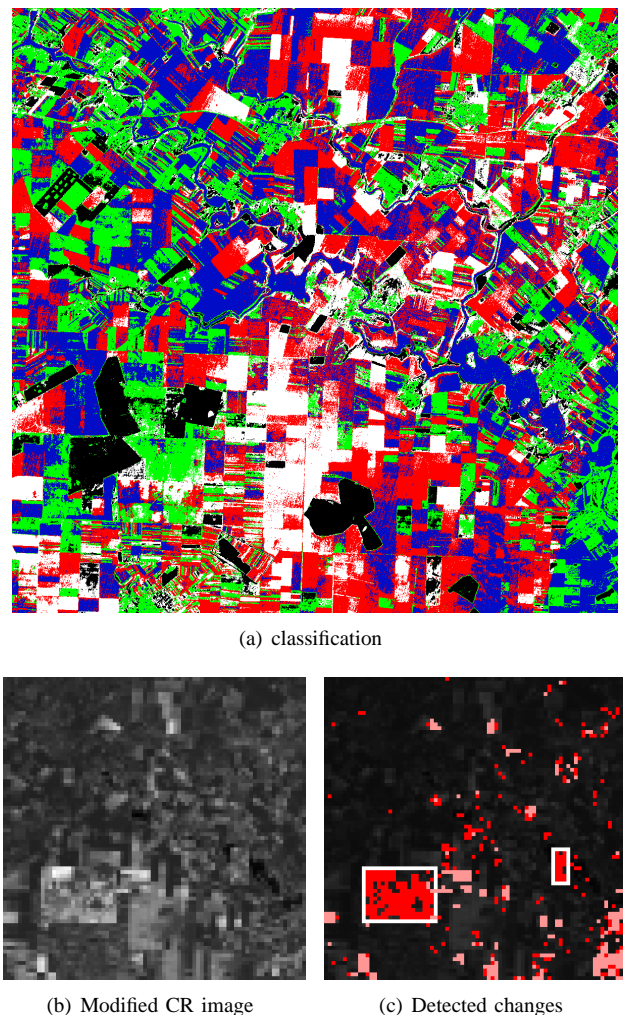


Fig. 3. Detection of changes introduced in the CR image (b) corresponding to the HR classification (a) : detected changes are represented in red Figure (c) and the boundary of introduced changes is represented in white in the same image. Changes concern 5.46% of the CR pixels and 96.2% of the image had been validated before introducing changes. Detected pixels concern 89.3% of the pixels, which is close to the expected 90.7%.

been proposed. This extension takes into account the fact a time series often shows high variabilities between two dates.

This new model enables the development of a fully unsupervised method for subpixelic change detection. The results obtained using pseudo-actual data showed very good performance and robustness to the resolution ratio used. However, further validation on actual time series with known changes are still to be performed, in order to analyse in particular the sensitivity of the model to misregistration errors and to other departures from the linear mixture model.

Moreover, this approach is based on the assumption of perfect image registration. Further work should focus on a registration sensitivity analysis as, in reality, registration is not perfect and the use of time series misregistered time series would lead to cumulated errors.

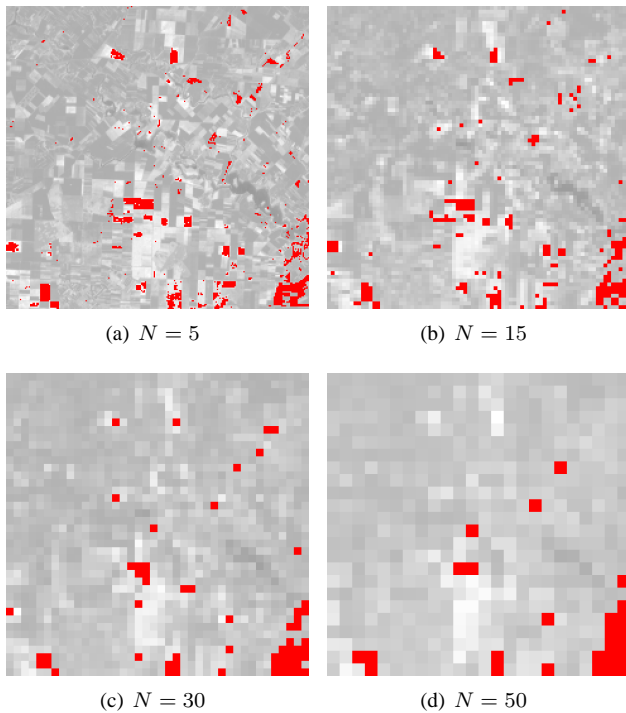


Fig. 4. Change detection using the HR classification of Figure 3 (a) and a CR image with a resolution ratio ( $N$ ) of  $5 \times 5$ ,  $15 \times 15$ ,  $30 \times 30$  and  $50 \times 50$ . Detected pixels are presented in red, superimposed on the CR image used.

#### ACKNOWLEDGMENT

The authors would like to thank the Centre National d'Études Spatiales (CNES) for providing the ADAM data base. A. Robin has been funded by a grant from the CNES and Astrium/EADS.

#### REFERENCES

- [1] H. Horwitz, R. Nalepka, P. Hyde, and J. Morgenstern, "Estimating the proportions of objects within a single resolution element of a multi-spectral scanner," in *Proceedings of the 7th International Symposium on Remote Sensing of Environment.*, Ann Arbor, Michigan, 1971, pp. 1307–1320.
- [2] A. Desolneux, L. Moisan, and J. Morel, "Meaningful alignments," *Int. J. Comp. Vision*, vol. 40, no. 1, pp. 7–23, 2000.
- [3] A. Desolneux, L. Moisan, and J.-M. Morel, *From Gestalt Theory to Image Analysis - A Probabilistic Approach*, Springer, Ed., 2007.
- [4] W. Malila, "Change vector analysis: an approach for detecting forest changes with landsat," in *Proc. of the Annual Symposium on Machine Processing of Remotely Sensed Data*, 1980, pp. 326–335.
- [5] E. Lambin and A. Stralher, "Change vector analysis in multitemporal space: a tool to detect and categorize land-cover change processes using high temporal-resolution satellite data," *Remote Sensing of Environment*, vol. 48, pp. 231–244, 1994.
- [6] P. Coppin, I. Jonckheere, K. Nackaerts, B. Muys, and E. Lambin, "Digital change detection methods in ecosystem monitoring: a review," *International Journal of Remote Sensing*, vol. 25, no. 9, pp. 1565–1596, May 2004.
- [7] A. Robin, "Détection de changements et classification sous-pixeliques d'images satellitaires. application au suivi des surfaces continentales." Ph.D. dissertation, Université Paris Descartes, France, 2007.
- [8] M. Fischler and R. Bolles, "Random sample consensus: a paradigm for model fitting with applications to image analysis and automated cartography," *Communications of the ACM*, vol. 24, pp. 381–385, 1981.

- [9] S. Le Hégarat-Masclé and R. Seltz, "Automatic change detection by evidential fusion of change indices," *Rem. Sens. Environment*, vol. 91, pp. 390–404, 2004.
- [10] A. Robin, S. Le Hégarat-Masclé, and L. Moisan, "A multiscale multi-temporal land cover classification method using a bayesian approach." Bruges: SPIE Remote Sensing, 2005.